

# Semi-Synthetic Sialic Acid Probes for Challenging the Substrate Promiscuity of Enzymes in the Sialoconjugation Pathway

Alexander Mertsch,<sup>a</sup> Silvan Poschenrieder,<sup>a</sup> and Wolf-Dieter Fessner<sup>a,\*</sup>

<sup>a</sup> Institute of Organic Chemistry and Biochemistry, Technische Universität Darmstadt, Alarich-Weiss-Str. 4, 64287 Darmstadt, Germany  
Tel: +49 6151 1623645  
Fax: +49 6151 1623645  
E-mail: fessner@tu-darmstadt.de

Manuscript received: July 21, 2020; Revised manuscript received: September 14, 2020;  
Version of record online: October 19, 2020

Supporting information for this article is available on the WWW under <https://doi.org/10.1002/adsc.202000859>

© 2020 The Authors. Published by Wiley-VCH GmbH. This is an open access article under the terms of the Creative Commons Attribution Non-Commercial License, which permits use, distribution and reproduction in any medium, provided the original work is properly cited and is not used for commercial purposes.

**Abstract:** A series of unusual sialic acid analogs were prepared using a semi-synthetic strategy. Truncation of natural *N*-acetylneuraminic acid was followed by diastereoselective carbon backbone reconstruction using Barbier-type carboligations as well as different functional group interconversions, which provided access to a variety of functional motifs in the terminal carbon backbone, including examples of saturated and unsaturated, linear and branched alkyl chains, partially deoxygenated sialic acids, sialic diacids and a first truncated legionaminic acid analog. The synthetic sialic acid probes were studied for nucleotide activation by the CMP-sialic acid synthetase from *Neisseria meningitidis* using a universal pH-shift assay for kinetic analysis. One-pot enzymatic nucleotide activation and sialyltransfer to lactose was performed using a selection of five probes together with an engineered  $\alpha$ 2,3-sialyltransferase from *Photobacterium phosphoreum* to furnish five new-to-nature analogs of the GM3 trisaccharide, which were finally utilized to test the substrate tolerance of two bacterial sialidases. The obtained set of sialic acid analogs and neo-sialoconjugates provides interesting opportunities for further glycobiology studies.

**Keywords:** Barbier-type reaction; Glycoconjugates; *N*-Acetylneuraminic acid; Semi-synthesis; Sialyltransfer

## Introduction

Sialic acid (Sia) is a generic term for members of a large family of  $\alpha$ -keto acid sugars with a nine-carbon backbone. Sias are omnipresent in vertebrates as the outermost glycan residues of cell-surface glycoproteins and glycolipids, with 5-acetamido-*D*-glycero-*D*-galactato-2-nonulosonic-acid (*N*-acetylneuraminic acid, Neu5Ac, **1**) being the most abundant.<sup>[1–2]</sup> For specificity in biological recognition the structural complexity of sialoconjugates is further enhanced post-glycosylation via *N*- or *O*-modification of natural Neu5Ac. An outstanding diversity is generated by acetylation, methylation, lactoylation, phosphorylation, sulfation and intramolecular lactam or lactone formation, with over 50 natural derivatives identified so far.<sup>[3]</sup> Some related

9-deoxygenated 5,7-bisamido analogs, such as legionaminic acid or the diastereoisomer pseudaminic acid, can be found in certain pathogenic bacteria (Figure 1).<sup>[4–5]</sup> Sialoconjugate complexity is directly associated with their numberless functions in biological recognition phenomena, such as immune regulation, inflammation, signaling, blood coagulation, fertilization, cell-cell adhesion, growth and differentiation.<sup>[6–8]</sup>

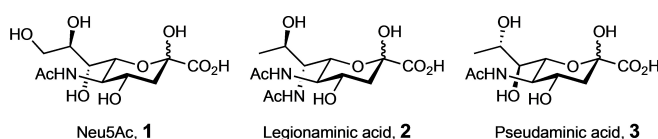


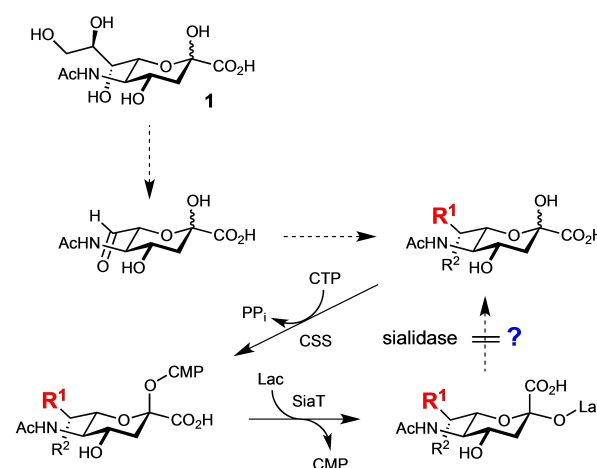
**Figure 1.** Important naturally occurring sialic acid structures.

Sia recognition by siglecs (sialic acid binding immunoglobulin-like lectins) mediates regulatory functions in the immune system and provides opportunities for innovative therapeutic strategies against a wide range of immunological disorders or cancer.<sup>[9]</sup> Identification and synthesis of high affinity sialoside ligands continue to be an important topic in immune cell-targeting therapy strategy, because they can outcompete natural siglec ligands.<sup>[7,10]</sup> Selective siglec targeting was attempted by studying their modulated affinity against variations of the Sia structure at positions C4, C5 and C9, and successfully achieved for discrimination of sialoadhesin (siglec-1),<sup>[11]</sup> CD22 (siglec-2),<sup>[12–13]</sup> CD33 (siglec-3),<sup>[14]</sup> myelin-associated glycoprotein (siglec-4),<sup>[15]</sup> and others.<sup>[16–17]</sup>

Viral and bacterial sialidases (or neuraminidases) that catalyze the cleavage of terminal sialic acid residues from sialylated glycolipids and glycoproteins are also attractive targets for pharmaceutical developments.<sup>[18]</sup> Sialidases are critical enzymes that provide human pathogenic bacteria with a sialic acid source and facilitate colonization and infection of the host,<sup>[19]</sup> which renders designed inhibitors as potent antimicrobial therapeutics. Sialidase inhibitors such as Oseltamivir, Zanamivir or natural products (e.g., siastatin B) were shown to be successful antiviral drugs and/or potential antibacterial agents.<sup>[20]</sup> However, the substrate and inhibitor specificity profiles of sialidases was less well studied, despite their use as important analytical tools, and hence depends on the synthetic availability of Sia analogs and their glycoconjugates.

Functional modification of the terminal Neu5Ac carbon chain, for example by acylation, sulfation or methylation of 7-, 8- or 9-O, is known to have striking effects on biological recognition phenomena, including microbe-host interaction, regulation of immune response, cellular apoptosis and tumor immunology. Recently, several sialoconjugates were prepared carrying functional modifications at the C7, C8 or C9-position in the Sia unit to study their influence on high-affinity selectin binding, sialidase resistance, or viral attachment.<sup>[21–23]</sup>

Conventionally, Sia derivatives are synthesized chemo-enzymatically by using *N*-acetylneuraminic acid aldolase (NeuA) for pyruvate addition to derivatives and analogs of *N*-acetylmannosamine.<sup>[22]</sup> However, this approach limits the scope of Sia variation by the enzyme's substrate specificity that requires polyhydroxylated precursors of at least the size of pentose. Here we present a complementary semi-synthetic strategy towards Neu5Ac structure variation based on selective truncation of the C7–C9 carbon chain followed by novel stereoselective chain re-construction. Our strategy allows the introduction of non-natural levels of functionalization that are difficult or impossible to access by simple functional group modification of natural **1** (Scheme 1). We demonstrate



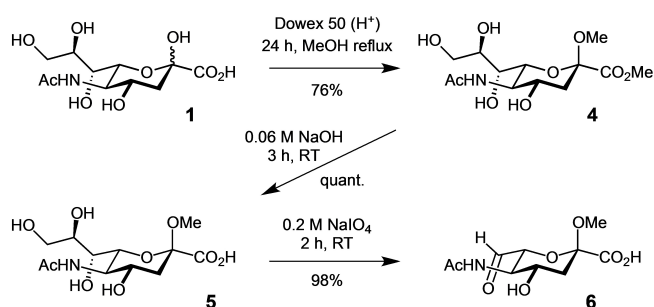
**Scheme 1.** Synthetic strategy toward terminally modified sialic acids, their use for biocatalytic synthesis of neo- sialoconjugates along the Leloir pathway, and potential sialidase inhibition.

that such unusual Sia analogs can be activated by CMP-sialate synthetase (CSS: *N*-acetylneuraminyl cytidyltransferase, E.C. 2.7.7.43) from *Neisseria meningitidis*<sup>[24–26]</sup> as a precondition for sialyltransfer by an engineered  $\alpha$ 2,3-sialyltransferase variant from *Photobacterium phosphoreum*,<sup>[27]</sup> and that the resulting neo-sialoconjugates show partial resistance against sialidase activity.

## Results and Discussion

**Novel semi-synthetic route to Neu5Ac analogs.** Our synthetic strategy is based on the indium-mediated addition of allylic reagents to the truncated Neu5Ac-derived C7-aldehyde (**6**) to reconstitute the Sia backbone. This was expected to yield homoallylic alcohols that provide various options for subsequent chemo-, regio- and stereoselective chemical modification for an access to structure motifs comprising different polarity, spatial demand and functional diversity. Barbier-type addition of organoindium reagents to reactive carbonyl compounds can be conducted in water under environmentally benign conditions and tolerates a wide array of functional groups precluding any need for protection-deprotection tactics as otherwise typical in carbohydrate chemistry.<sup>[28–29]</sup> Such carbonylation reactions proceed at convenient rates under ambient temperature with high yield and afford good diastereoselectivity with the help of chelation control.<sup>[30]</sup> Compound **6** was readily accessible from commercial Neu5Ac in good overall yield via three scalable steps following a literature procedure (Scheme 2),<sup>[31]</sup> and offered to be a flexible starting material also for other functional group interconversions.

With a relatively low first ionization potential, indium supports the mildest reaction conditions as



**Scheme 2.** Synthesis of C<sub>7</sub>-aldehyde precursor **6** by oxidative degradation of Neu5Ac (**1**).

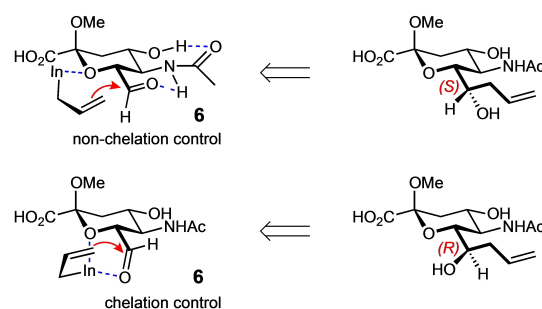
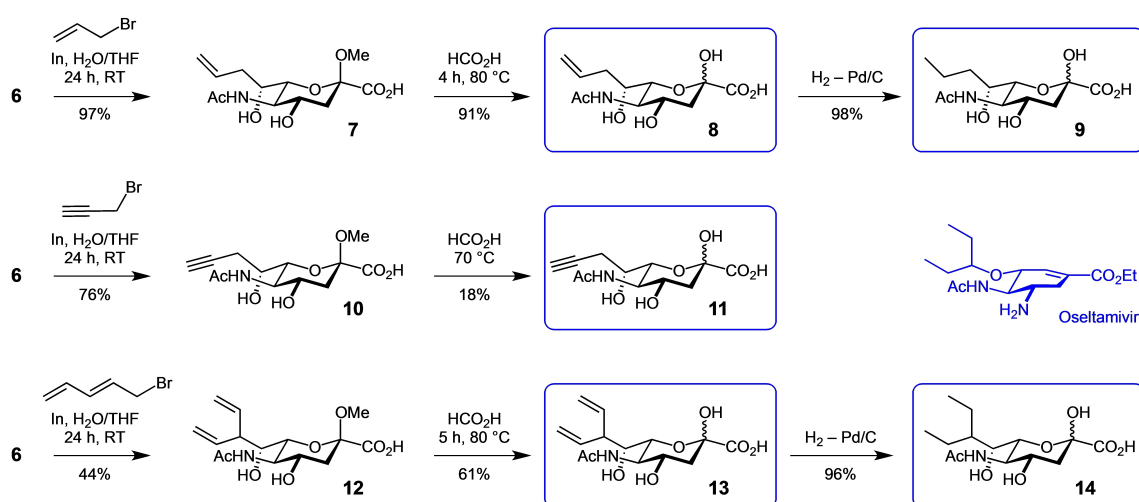


**Figure 2.** π-Facial stereocontrol for indium-mediated allyl transfer to aldehyde **6**; intramolecular carbonyl pre-orientation by hydrogen bonding *versus* reagent based chelation effect.

compared to zinc and tin mediated Barbier-type additions, which are best performed in more demanding acidic media such as in the presence of NH<sub>4</sub>Cl (Zn) or mineral acid (Sn) for activation.<sup>[32]</sup> Indeed, when the sterically demanding aldehyde **6** was subjected to allylbromide addition in the presence of In(0) at room temperature (Scheme 3), higher conversion rates and higher yields of product **7** were obtained in comparison to corresponding Zn(0) reactions. Ultrasonication assisted in a quick reaction start and progress, which could be further accelerated by the addition of a catalytic quantity of InCl<sub>3</sub>. Three complementary bromide reagents were used for indium mediated allylation, propargylation and pentadienylation in aqueous solution, using 50% THF to enhance the solubility. For unsubstituted allyl fragments the addition of the generated allylindium reagent to the carbonyl compound usually proceeds exclusively at the γ-position of the allyl halide in an S<sub>N</sub>2' manner;<sup>[29]</sup> in case of the pentadienyl reagent this γ-regiospecificity led to the formation of the branched-chain nonconju-

gated homoallylic alcohol **12** as the sole product. For propargylic reagents, an equilibration of propargyl- and allenylmetal species by a metallotropic rearrangement explained the almost exclusive formation of the homopropargylic alcohol product (**10**). The individual product yields varied from almost quantitative with allylbromide (97% **7**), good with propargylbromide (76% **10**) to acceptable (44% **12**) with the sterically demanding pentadienylbromide reagent (incomplete conversion within 24 h).

Interestingly, under these conditions only a single diastereomeric product was obtained with all three allylic reagents according to NMR analysis. A high level of stereocontrol was to be expected due to the rigid ring conformation of aldehyde **6**. Conceptually, two alternative models may account for π-facial stereocontrol in the addition step (Figure 2): (i) if the aldehyde carbonyl was pre-oriented to the neighboring amide group by intramolecular hydrogen bonding, this would result in nucleophilic attack from the sterically least hindered hemisphere, generating the (S)-configu-



**Scheme 3.** Synthesis of sialic acid analogs based on indium mediated *Barbier* type chain extension, and structural relationship of the branched 3-pentyl motif to anti-influenza drug *Oseltamivir*.

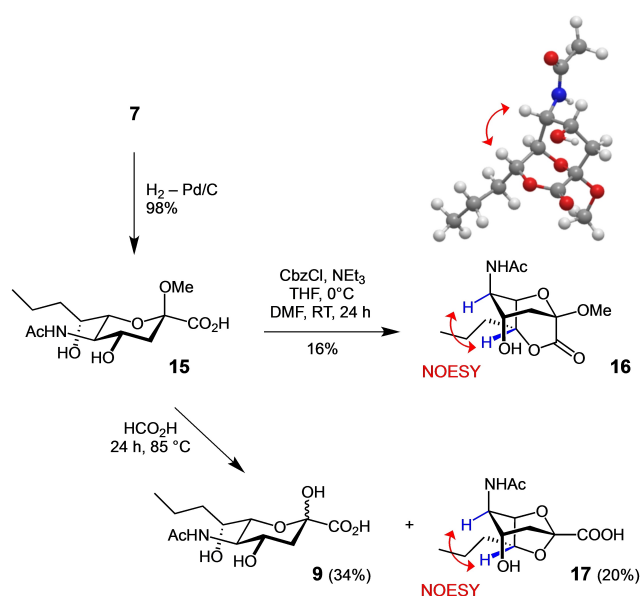
rated carbinol, or (ii) if  $\beta$ -chelation of the indium reagent by both aldehyde carbonyl and the ring O-atom was operative, this would direct the attack to occur from the less hindered opposite  $\pi$ -face, resulting in the (*R*)-configured carbinol. Complexation of the indium reagent by the axial oxygen lone pair would be further supported by the anomeric effect. Even in aqueous solution, chelation was shown to be a dominant factor for  $\pi$ -facial stereocontrol in acyclic  $\alpha$ -oxygenated aldehydes,<sup>[33–34]</sup> leading predominantly to *syn* products (corresponding here to an absolute (*R*)-configuration).

For an unambiguous determination of the configuration at C7, rigid vicinal orientation was desirable *via* intramolecular formation of the Sia 1,7-lactone **16**. After double bond saturation to avoid elimination, lactone formation was induced in **15** by chemoselective activation of the carboxylic acid group with mildly reactive benzyloxycarbonyl chloride (CbzCl), which does not react with secondary hydroxyl groups.<sup>[35]</sup> If the configuration at C7 is (*R*), there would be a positive correlation between the spatially close protons at C5 and C7 (Scheme 4), as anticipated for chelation-controlled addition and as present in natural Neu5Ac. Indeed, NOESY NMR analysis of bicyclic lactone **16** clearly showed positive cross-peaks between proton signals of 5-H and 7-H, proving their fixed spatial *syn*-orientation and thus absolute (*7R*)-configuration in product **7**. Spectral comparison with similar vicinal coupling patterns for 6- and 7-H within all *Barbier* reaction products (**7**, **10** and **12**) further confirmed that these compounds were generated

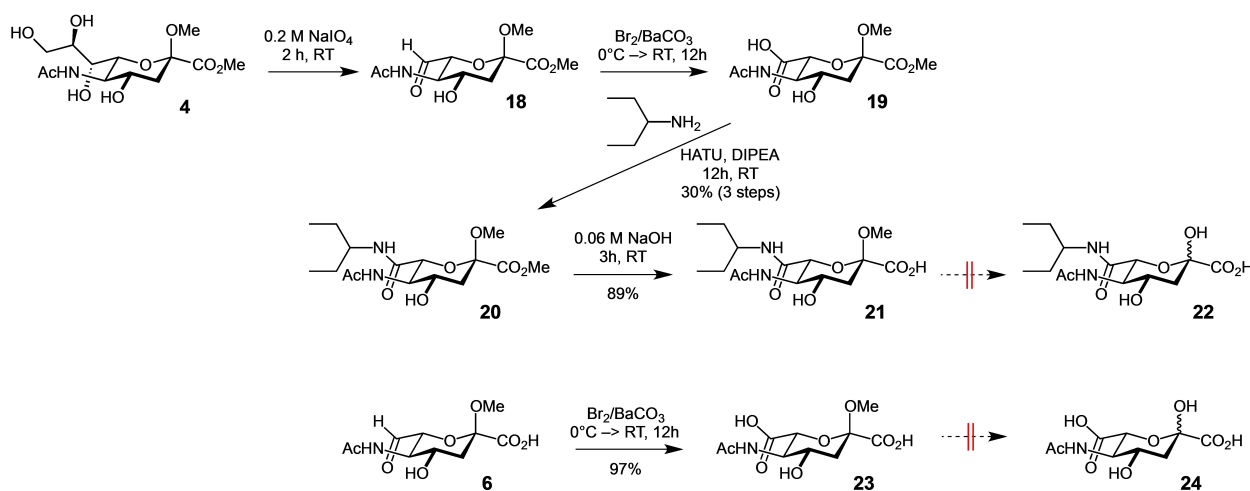
consistently *via* identical chelation-controlled allylation/propargylation pathways. Interestingly, partial intramolecular 2,7-transacetalization occurred upon the attempt to deprotect the glycosidic acetal in **15**, furnishing **17** along with the expected free Sia analog **9**. NOESY analysis of **17** also confirmed the (*7R*)-configuration by 5-H/7-H cross-peaks. It is noteworthy that 2,7-acetal Sia structures with specific C5-*N*-substitution are selective micromolar inhibitors against certain bacterial sialidases.<sup>[36–37]</sup>

Deprotection of the semi-synthetic Sia analogs was conducted with aqueous formic acid according to a published protocol.<sup>[31]</sup> Depending on the substitution pattern, reaction temperature and time had to be adjusted to achieve full conversion to free Sia analogs **8**, **9**, **11** and **13**. Nevertheless, yields varied significantly and interestingly benefited from unsaturation since allyl and pentadienyl compounds gave good yields, whereas the corresponding hydrogenated derivatives were more reluctant and yields dropped dramatically. Therefore, hydrogenation to saturated Sia analogs **9** and **14** had to be performed after acetal hydrolysis. No improvement was achieved by using a series of other acids or solvent mixtures. A possible explanation may be related to the ease of 1,7-lactone or 2,7-acetal formation in view of the reported instability of lactones that was found responsible for eminent loss of material in related cases.<sup>[35]</sup> Compounds **8**, **9**, and **11** derived from allylation and propargylation share a C<sub>10</sub> backbone structure but miss hydroxylation at positions C8 and C9. These compounds have a spatial demand similar to Neu5Ac, but very different polarity and display an increasing rigidity in parallel to their degree of unsaturation. The pentadienyl analog **13** and saturated **14** show a branched structure motif, which is similar in size and polarity to that present in the well-known antiviral drug *Osetamivir* (**17**) used for influenza treatment.<sup>[20]</sup> Corresponding derivatives or even conjugates of **13/14** themselves promise to have sialidase inhibitory activity as suggested by their significant structural similarity.

A second set of Sia analogs was pursued by aldehyde oxidation to the corresponding acid, which offers facile access to structural diversification via amide formation. Because such an approach required full C1/C2 protection, compound **4** was first truncated by diol cleavage to give aldehyde **18**, then oxidized to the C7-carboxylic acid derivative **19** (Scheme 5).<sup>[38]</sup> Exemplary amide coupling with 3-pentylamine was performed with HATU to give the amide **20** in 3 steps with 30% overall yield. Much to our surprise, removal of the anomeric protection in **21** could not be effected under standard acidic conditions and the material decomposed upon more forcing treatment. The *N*-(3-pentyl)amide motif of **22** would have been an interesting probe corresponding to **14** and *oseltamivir*, in particular since related *N,N*-dialkylamides were



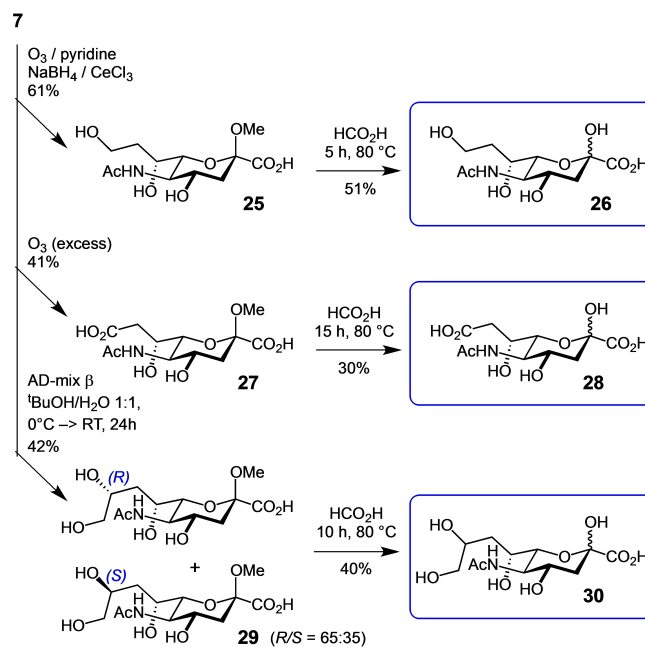
**Scheme 4.** Intramolecular 1,7-lactone formation (**16**; structure model shown at top right) and unexpected intramolecular acetal formation (**17**) allowed unambiguous configurational analysis.



**Scheme 5.** Synthetic routes to C7-carboxylic acid analogs of Neu5Ac. Anomeric deprotection of *N*-(3-pentyl)carboxamide **23** and the corresponding C7-carboxylic acid **21** was unsuccessful.

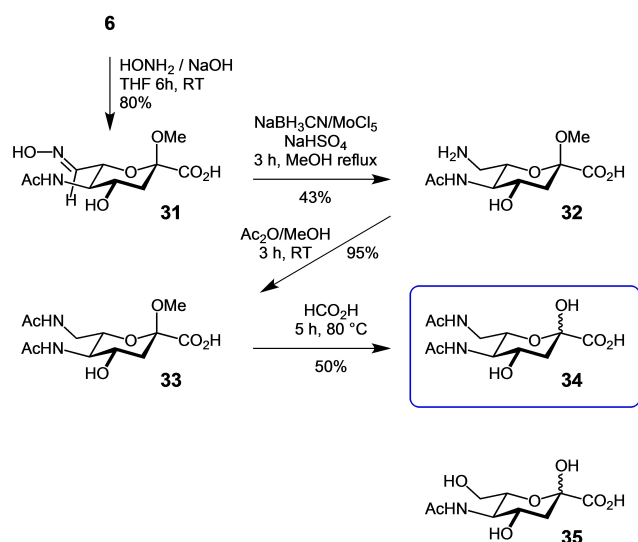
recently produced by a complementary carboligation approach as a potential neuraminidase inhibitors, albeit with low diastereoselectivity.<sup>[39–40]</sup> As a control experiment, aldehyde **6** was oxidized to C7-carboxylic acid derivative **23** to be subjected to various deprotection conditions. However, again all attempts for anomeric deprotection failed or led to decomposition. This is quite puzzling as **6** could be easily deprotected under mild conditions. Possible explanations might be that the electron-withdrawing properties of C7-carboxylic moieties are destabilizing the forming glycosyl cation, and/or that a C7-carbinol moiety might offer anchimeric assistance in the deprotection step via trans-acetalization as evidenced by the formation of **17**. Clearly, standard anomeric protection turned out to be a limiting factor for the chosen synthetic strategy depending on the oxidation level of the carbon backbone. Nevertheless, sialosides **21** and **23** are of interest as potential high-affinity ligands for Siglecs.<sup>[13,41]</sup>

The allyl motif in readily accessible platform compound **7** was used for further development of discriminating functionalization (Scheme 6). Controlled ozonolysis in the presence of catalytic pyridine<sup>[42]</sup> followed by reductive work-up furnished the glycoside **25**, which was deprotected to give 8-deoxy-Neu5Ac. Excess ozone resulted in terminal overoxidation to **27**, which was deprotected to yield the 8-deoxy-9-carboxylate derivative **28**. Dihydroxylation of **7** was pursued to get access to a Sia mimetic with an extended C<sub>10</sub> backbone. Standard dihydroxylation with OsO<sub>2</sub>(OH)<sub>4</sub> led to a 50/50 mixture of C9-diastereomers **29** as expected. Attempts at selective asymmetric dihydroxylation using the *Sharpless* AD-mix β only gave a 65:35 (*R/S*) mixture, from which individual stereoisomers could not be separated by standard silica chromatography. Deprotection provided the free Sia analog **30**.



**Scheme 6.** Functionalization of the allyl motif in platform compound **7** toward different oxygenation levels.

Reductive amination of aldehyde **6**, e.g. with bulky adamantylamines, was described as a route towards potential antiviral compounds.<sup>[31]</sup> In a complementary manner, we targeted the amine **32** as a precursor to truncated analogs of legionaminic acid **2** carrying an acetamido substituent at the C7 position. To this end, the oxime **31** (Scheme 7) was unsuccessfully subjected to common reduction methods using ammonium formate and zinc,<sup>[43]</sup> sodium borohydride in different solvents, hydrogenation with palladium on coal or with platinum oxide at elevated pressure (17 bar).<sup>[44]</sup> Therefore, recourse was made to reduction with sodium



**Scheme 7.** Synthesis of truncated C<sub>7</sub>-analog of legionaminic acid **35**.

cyanoborohydride and molybdenum chloride as a catalyst,<sup>[45]</sup> which furnished the desired amine **32**. Exemplary acylation with acetic anhydride (**33**) and deprotection under standard conditions produced the diacetamido derivative **34**. The truncated C<sub>7</sub>-Sia **35** was prepared as a control compound for comparison purposes by reduction/deprotection of aldehyde **6**.<sup>[25]</sup>

**Kinetic Screening of CSS activity with Neu5Ac analogs.** Successful synthesis of *neo*-sialoconjugates critically depends on the nucleotide activation of Sia analogs by CSS as the key step. CSS substrate binding occurs in a deep cleft via an induced-fit mechanism that encloses the entire substrate structure. In contrast, most sialyltransferases required for the consecutive conjugation step display a rather shallow binding pocket for the Sia moiety that tolerates structural modifications quite well. Therefore, a kinetic assessment of the influence of alterations in the Sia structure on the CSS activity was important, whereas the kinetics for sialyltransfer were judged to be less significant. To evaluate the kinetic properties of the newly produced Neu5Ac analogs a colorimetric pH-sensitive assay previously developed by our group was used.<sup>[25–26]</sup> Briefly, a stoichiometric equivalent of pyrophosphoric acid is released upon nucleotidyl transfer from substrate CTP to give CMP-Sia, and the resulting pH shift can be quantified in the presence of a pH indicator for continuous monitoring of the reaction progress. Nine newly synthesized Neu5Ac analogs were kinetically analyzed in microtiter plate format for conversion by CSS from *Neisseria meningitidis* using this assay principle (Table 1). The parent Sia **1** and its truncated C<sub>7</sub> analog **35** were included for reference. The analysis confirmed the unusually broad substrate promiscuity of the *N. meningitidis* CSS

**Table 1.** Apparent steady-state kinetic parameters<sup>[a]</sup> for substrate analogs of CSS

Compd	$K_M$ [mmol]	$k_{cat}$ [1/min]	$k_{cat}/K_M$ [mM <sup>-1</sup> min <sup>-1</sup> ]
<b>1</b>	0.15 ± 0.03	647 ± 37.1	4227
<b>8</b>	0.07 ± 0.02	120 ± 7.4	1745
<b>9</b>	0.18 ± 0.04	112 ± 5.8	643
<b>11</b>	0.14 ± 0.03	161 ± 7.8	1117
<b>13</b>	0.25 ± 0.06	372 ± 23.9	1462
<b>14</b>	0.17 ± 0.04	123 ± 7.2	726
<b>26</b>	0.03 ± 0.01	127 ± 9.8	4441
<b>28</b>	1.60 ± 0.62	132 ± 15.2	83
<b>30</b>	0.76 ± 0.43	98 ± 10.3	130
<b>34</b>	0.04 ± 0.01	74 ± 3.7	1917
<b>35</b>	0.035 ± 0.01	54 ± 3.7	1527

<sup>[a]</sup> Data were determined by colorimetric pH-sensitive assay by varying the concentration of Sia substrates under standard conditions (0.5 mM CTP, 10 mM MgCl<sub>2</sub>, 0.026 mM kresol red, 1.27 μg CSS) followed by Michaelis-Menten analysis.

because all tested substrate analogs were converted by the enzyme. While previous work had mostly focused on structural variations of the amide moiety, chain truncation and stereochemical variations of the hydroxylation pattern, our current study shows that also constitutional modifications of the carbon backbone, unsaturated or fully deoxygenated as well as chain extended derivatives are tolerable.

CSS binding affinity seems to be strongly related to polarity changes at the terminal sugar chain. Interestingly, C<sub>8</sub> deoxygenation in **26** resulted in the strongest binding affinity among all compounds tested with a more than 5-fold lower  $K_M$  value relative to Neu5Ac (**1**), however, compensated by a corresponding 5-fold loss in  $k_{cat}$ . Having the same structure motif but extended by an additional hydroxymethylene group, compound **30** showed 26-fold lower affinity and 34-fold lower relative catalytic efficiency, indicating that the active site space of CSS in this region is very limited. Gratifyingly, all hydrophobic *Barbier* products (**8**, **11**, **13**) and their hydrogenated derivatives (**9**, **14**) displayed affinities in the range of the native Neu5Ac with rather minor variations. The allyl group in **8** seemed to fit best, while the bulky and rather rigid pentadienyl moiety in **13** may present some conformational difficulties. Remarkably, both unsaturated compounds (**8**, **13**) displayed at least 2-fold higher catalytic efficiency when compared to the corresponding saturated structures (**9**, **14**). As was to be expected from our earlier CSS studies with non-natural Sia derivatives,<sup>[25,26]</sup> all synthetic analogs showed reduced  $k_{cat}$  values in comparison to the natural substrate Neu5Ac. On the other hand, substrate **28** carrying a charged carboxylate in 9 position showed the lowest binding affinity of all probes and >50-fold lower catalytic efficiency relative to the parent Neu5Ac.

Conversely, the truncated analogs **34** and **35** showed excellent binding affinity but the lowest turnover numbers. Apparently, a second acetamide moiety present in **34** could not compensate for the loss of the natural hydroxylated backbone.

Our substrate binding model<sup>[25]</sup> from structural alignment of the CSS from *N. meningitidis* (PDB entry 1EYR)<sup>[46]</sup> and the corresponding murine enzyme (PDB entry 1QWJ)<sup>[47]</sup> was consulted for an interpretation of the kinetic discrimination of substrate analogs (Figure 3). The CSS mechanism involves an intricate hydrogen bond network that correctly controls the positions of the sialic acid, nucleoside triphosphate and divalent ions in the highly polar transition state of nucleotidyl transfer. Earlier data suggested that substrate alterations such as carbinol stereoinversion or deoxygenation, which perturb the hydrogen bond network, lead to significant reduction in  $k_{cat}$ .<sup>[25]</sup> We previously hypothesized that the loss of a hydrogen bridge between Gln104 to 8-OH might cause a conformational change of the Gln104 side chain to an orientation that might interfere with the catalytic activation of the O-2 nucleophile.<sup>[25]</sup> The results with the newly produced derivatives all lacking the 8-OH group support this hypothesis. All of them show

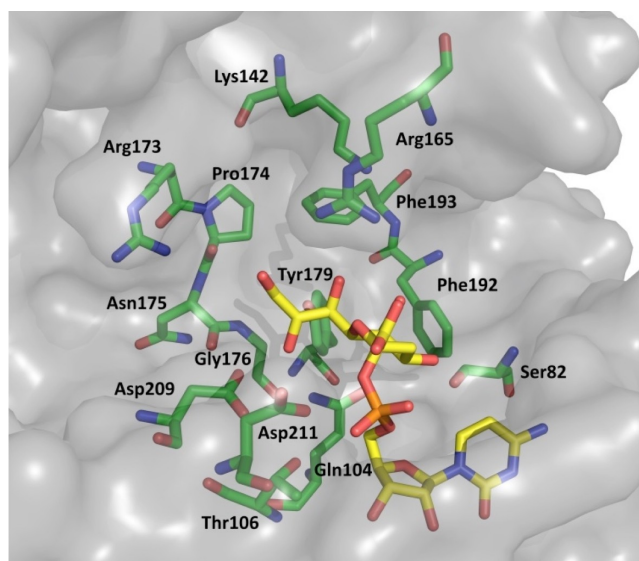


**Figure 3.** Model of CMP-Neu5Ac binding in the crystal structure of CSS showing the binding environment for the sialic acid C7–C9 chain.<sup>[25]</sup> The carbon backbones are shown in green for active site residues within the sialic acid pocket of CSS from *Neisseria meningitidis* (PDB entry 1EYR)<sup>[46]</sup> assumed to be involved in substrate binding. Carbon skeleton of bound substrate CMP-Neu5Ac is displayed in yellow and modeled in the same conformation as determined from the murine CSS structure (PDB entry 1QWJ).<sup>[47]</sup> The substrate was docked by alignment of both protein folds and by weighted corrections considering the mononucleotide portion of the substrates. The figure was prepared with the aid of PyMOL.

reduced  $k_{cat}$  values consistent with a disturbance of the hydrogen-binding network, specifically with Gln104 or Asp211, whereas most  $K_M$  values are similar to that of the natural substrate. Therefore, 8-OH seems to contribute less to the binding energy but mostly impacts  $k_{cat}$ . Interestingly, despite rigidity and steric bulkiness of unsaturated backbone structures or their hydrophobic nature, the analogs seem to be tolerated quite well in a pocket that is not really non-polar except for Pro174. The worst binding affinity found for **28** might be due to its 9-carboxylate group, which seems to be pointing directly towards non-polar Pro174.

To verify the consequences from the kinetic study, substrate analogs **8**, **11**, **13** and **34** were used in a one-pot two-enzyme cascade (Scheme 1) on a preparative scale. Nucleotide activation was performed by wild-type CSS from *Neisseria meningitidis* followed by sialyltransfer to lactose using an engineered variant of the  $\alpha$ 2,3-sialyltransferase from *Photobacterium phosphoreum* (2,3SiaT<sub>pph</sub>\_A151D) with significantly reduced hydrolysis activity. The relative reaction progress and sialoconjugate yields were compared to that of a positive control, which used Neu5Ac for synthesis of the natural GM3 trisaccharide (Neu5Ac-Lac, **36**). First, all Sia compounds (40 mg each, >0.1 mmol) were incubated with 1.5 eq of CTP in the presence of CSS and inorganic pyrophosphatase and monitored by TLC. 3-Pentadienyl analog **13** showed completion already after 2 hours, allyl (**8**) and propargyl (**11**) compounds required 3.5 hours, whereas the acetamido derivative **34** was still incomplete after 5.5 hours, which matches the kinetic data from the assay quite well. After addition of 3 eq lactose, reaction mixtures were incubated with  $\alpha$ 2,3-SiaT<sub>pph</sub>\_A151D for additional 24 h. Products (Figure 4) were purified by size exclusion chromatography and lyophilized. Relative to **36** (91%), the isolated yields of the corresponding allyl (**37**, 80%), propargyl (**38**, 92%) and 3-pentadienyl (**39**,

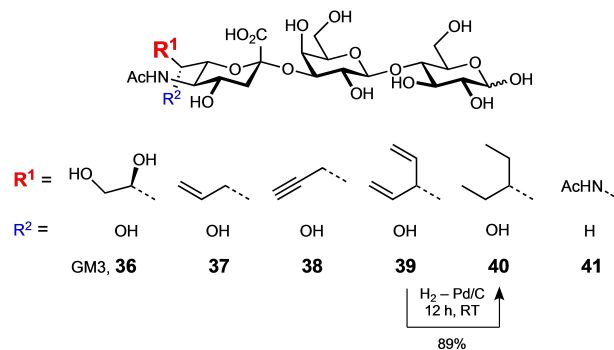
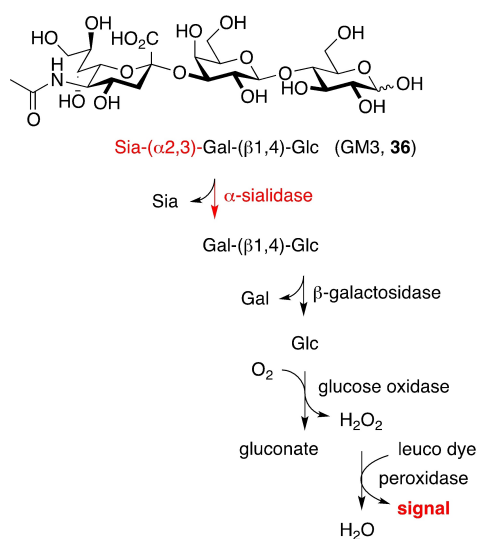


**Figure 4.** GM3 trisaccharide (**36**) and analogs (**37–39**, **41**) prepared by enzymatic one-pot synthesis from lactose and newly synthesized Sia analogs according to Scheme 1; catalytic hydrogenation furnished the saturated GM3 analog **40**.

78%) analogs were highly satisfactory. To access the *Oseltamivir*-related branched 3-pentyl motif, trisaccharide **39** was saturated by catalytic hydrogenation to furnish **40**. The trisaccharide **41** derived from compound **35** was obtained with only 63% yield due to incomplete CMP-activation (30% of **34** recovered). However, compound **41** is interesting as a first analog of legionaminic acid containing oligosaccharides, which are yet difficult to prepare owing to a lack of easily accessible substrates and enzymes from the corresponding biosynthetic pathway.<sup>[48]</sup>

**Sialidase activity.** Viral and bacterial sialidases are common exo-glycosidases that play roles in pathogen infection of human hosts.<sup>[18]</sup> Sialidases from different sources vary in their preference in recognizing diverse sialic acid-containing structures. Sialosides conjugated to a fluorophore are commonly used to screen for sialidase activity, which increases the throughput of the assay but provides no information on the substrate specificity.<sup>[49–50]</sup> Thus, we used our small library of neo-sialoconjugates as convenient tools for studying the substrate specificity of sialidases by using a newly developed assay for continuous colorimetric determination of sialidase activity. In this coupled enzymatic assay (Scheme 8) individual sialosides were incubated with an appropriate amount of a sialidase of interest as well as excess amounts of  $\beta$ -galactosidase and glucose oxidase. If the GM3 analog is a suitable substrate, the sialidase activity will cleave the terminal sialic acid to liberate lactose. The excess amounts of auxiliary enzymes quickly produce a stoichiometric amount of hydrogen peroxide, which is detected via peroxidase-catalyzed formation of an equivalent quantity of a colored dye, which can be quantified using a microtiter plate reader.<sup>[51]</sup> Without the sialidase activity, no signal



**Scheme 8.** Coupled enzymatic assay for continuous colorimetric analysis of sialidase activity.

is detected because the galactosidase also acts as an exo-glycosidase that cannot hydrolyze internal galactosides.

In our first evaluation, two commercial bacterial sialidases ( $\alpha$ 2-3,6,8 neuraminidase) from *Clostridium perfringens* and *Vibrio cholerae* were tested. Data for modified Sia conjugates were normalized relative to the natural GM3 substrate as a reference (set to 100% activity; Figure 5). The sialidase of *C. perfringens* was moderately active with propargyl- (**38**), allyl- (**37**) and diacetamido-derivatives (**41**) at 44%, 43% and 7% relative activities, whereas the *V. cholerae* enzyme was almost inactive at 0.3%, 5% and 0% activity, respectively. Interestingly, the bulky but conformationally flexible 3-pentyl-derivative **40** showed the highest levels of activity (62 and 84%, respectively) with both bacterial enzymes. Apparently, this points to a significant and distinctive substrate binding geometry in comparison to the neuraminidase from influenza virus, for which oseltamivir is the structurally related target inhibitor. However, the latter enzyme was not available to us for a direct comparison. To briefly test for competitive binding affinities, a solution containing equal concentrations (4.0 mM) of GM3 and either **38** or **41** as the least active analogs was incubated with the *Vibrio* sialidase. The observed cleavage rate, which was about 20% reduced relative to pure GM3, indicates a rather moderate inhibition effect for the propargyl component, while the acetamide **41** did not show a noticeable competition against native GM3. Overall, our results reveal significantly higher substrate promiscuity of the *C. perfringens* sialidase with terminally hydrophobic Sia analogs, whereas in a related study with the enzyme from *V. cholerae* was somewhat more tolerant with analogs only modified at the 9-position.<sup>[52]</sup>

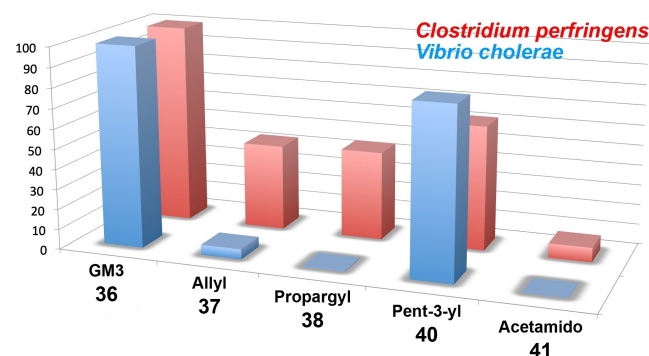


**Figure 5.** Relative activities of sialidases from *C. perfringens* and *V. cholerae* against neo-sialoconjugates **37**, **38**, **40** and **41** in comparison to native GM3 trisaccharide.



## Conclusion

Following a novel synthetic strategy based on the Barbier-type carbonylation of a chemically truncated Neu5Ac-derived C7-aldehyde, a series of unusual Sia analogs were successfully prepared in good yields. The method furnished the desired addition products with complete diastereoselectivity owing to indium-mediated chelation control and proceeded under environmentally benign conditions. The allyl adduct was converted into various Sia C<sub>9</sub>/C<sub>10</sub>-analogs by simple methods for exemplary functional group installation. Aldehyde **6** also proved a useful starting material for further functional group interconversions leading to the first truncated legionaminic acid C7-analog as well as amide derivatives of the C<sub>7</sub>-sialic diacid. It was noted that cleavage rates of methyl glycosides depend significantly upon the type of functionality at C7, where strong electron depletion causes resistance to acidic deprotection.

Ten Neu5Ac derivatives carrying different functional motifs in the terminal carbon backbone were studied for their responsiveness to CMP-activation by the CSS from *N. meningitidis* by kinetic analysis using a universal pH dependent assay. All new-to-nature analogs were found to be acceptable by this unusually tolerant CSS enzyme, although chain extension, truncation, and highly polar carboxylate groups strongly reduced both binding affinity and conversion rates. However, hydrophobic aliphatic moieties were converted quite well with only two- to five-fold reduction in  $k_{cat}$ . This could be demonstrated by one-pot activation and sialyltransfer to lactose on preparative scale using an  $\alpha$ 2,3-sialyltransferase variant  $\alpha$ 2,3-SiaT<sub>pph\_A151D</sub> engineered for reduced hydrolytic activity. The resultant GM3 trisaccharide and five novel analogs thereof, which were obtained in very good yields, were finally used to probe the substrate tolerance of two bacterial sialidases.

We believe that this novel allyl carbonylation-functionalization strategy is a versatile approach towards a pool of unusual Sia analogs by semi-synthesis, offering an access to a range of distinct functionalization levels that is difficult or impossible to be achieved by conventional routes for Sia synthesis. The set of synthetic Sia derivatives and analogs presented herein, as well as neo-sialoconjugates derived therefrom, will be of interest as synthetic probes for further glycobiological studies, including into their modulated affinity as immune cell-targeting ligands against siglec receptors.

## Experimental Section

**Materials and methods.** Neu5Ac was purchased from R&S Pharmchem, China. The CSS from *N. meningitidis* and the engineered  $\alpha$ 2,3-SiaT<sub>pph\_A151D</sub> from *P. phosphoreum* were

produced by recombinant expression and purified as described.<sup>[25,27]</sup> Cresol red and CTP were purchased from Carl Roth, Germany. Assays were measured using a SpectraMax 190 plate reader from Molecular Devices and *SoftMax Pro 6.5.1* software. Commercial reagents/solvents were used as received without further purification. Organic solvents were dried freshly by standard methods. Column chromatography was performed on *Roth* silica gel (0.040–0.063 mesh); analytical thin layer chromatography was performed on Merck silica gel plates 60 F<sub>254</sub> using anisaldehyde staining or *N*-(1-naphthyl)-ethylenediamine for detection. All R<sub>f</sub> values are reported for the TLC solvent mixture n-BuOH:acetone:H<sub>2</sub>O:AcOH = 35:35:23:7. Organic solvents were removed under vacuum using a rotary evaporator, and residues were dissolved in H<sub>2</sub>O and lyophilized. NMR spectra were recorded on Bruker DRX500 spectrometer; chemical shifts are referenced to HOD,  $\delta$  = 4.79 ppm. For quantitative NMR measurements an accurate manual phase correction and a baseline correction with Whittaker Smoother method were performed using MestReNova 11.0.3. High-resolution mass data were determined on a Bruker Impact II ESI-Q-TOF spectrometer.

**General procedure for Barbier-type reactions.** Aldehyde **6** (1 eq.) was dissolved in H<sub>2</sub>O:THF = 1:1 (v/v; 5 mL per 50 mg). Indium powder (2 eq., 200 mesh) and a catalytic amount of InCl<sub>3</sub> were added with vigorous stirring. The reaction was started by addition of a THF solution containing the respective allyl bromide (3 eq.), and the mixture was placed in an ultrasonic bath at RT. When TLC showed complete conversion, the reaction mixture was neutralized with 1 M NaOH, filtered through celite and the solvents were removed under vacuum. The residue was purified by silica column chromatography.

**General deprotection procedure for anomeric methoxy group.** Methyl glycosides were dissolved in H<sub>2</sub>O. Formic acid was added and the reaction mixture heated to 80 °C for 4–5 h. Conversion was checked by NMR analysis, because deprotection was difficult to follow by TLC, and the procedure repeated if necessary.

**Procedure for 1,7-lactone formation.** Solutions of NEt<sub>3</sub> (81.1 mg, 0.802 mmol, 1.24 eq.; 2.5 mL) and CbzCl (105.9 mg, 0.621 mmol, 0.96 eq.; 1.5 mL) in dry THF were combined at 0 °C, then **15** (197.4 mg, 0.647 mmol, 1 eq.) was added followed by DMF (3 mL). The mixture was allowed to warm up to RT with stirring for 24 h. When TLC showed complete conversion, the mixture was quenched by addition of methanol (4 mL). After standing for 2 hours all volatiles were removed under high vacuum.

**General procedure for the synthesis of  $\alpha$ 2,3-sialyllactoside analogs.** The respective Neu5Ac-derivative (40 mg) and CTP (1.5 eq.) were dissolved in Tris-HCl buffer (12 mL 50 mM, pH 8.5) containing 20 mM MgCl<sub>2</sub>. After addition of inorganic pyrophosphatase (10 U) the reaction mixture was re-adjusted to pH 8.5 and started by addition of 10 mg CSS from *N. meningitidis*, while keeping the pH constant by autotitration. After 2–3.5 h at 37 °C, when TLC analysis indicated the disappearance of the Neu5Ac derivative, lactose (3 eq.) and  $\Delta$ 24- $\alpha$ 2,3-SiaT<sub>pph\_A151D</sub> (0.5 mg) were added. After 22 h alkaline phosphatase (300 U) was added. When the conversion was completed (~27 h), an equivalent volume of cold methanol (–20 °C) was added to stop the reaction. Protein precipitate was

removed by centrifugation, methanol evaporated under reduced pressure, and the remaining solution directly purified over Biogel P-2 (Bio-Rad, Germany; 3 × 100 cm column). The product fractions were collected and lyophilized for NMR analysis.

**Enzyme kinetic parameters.** Components were pipetted consecutively into 96-well plates to give a total assay volume of 200 μL per well with following end concentration: Tris buffer (2 mM, pH 8.6; 75–175 μL), kresol red (2 μL, 10 mg L<sup>-1</sup>, 0.026 mM), substrate (Neu5Ac and analogs, 0–100 μL, 0–10 mM) and enzyme (3 μL; 1.27 μg). All solutions were carefully adjusted to pH 8.6 and tempered to 37 °C. The plate was shaken for ≈45 sec at 37 °C. The assay was started by addition of the constant substrate (20 μL freshly prepared CTP solution, 0.5 mM), the plate was immediately shaken again for 5 sec and then directly measured by plate reader (SpectraMAX 190; Molecular Devices, Software: SoftMax Pro 6.5.1) at 574 nm. Experimental data were fitted to the Michaelis-Menten equation by nonlinear regression using Origin software (v9.1G, OriginLab) to obtain kinetic parameters. Protein concentration was measured by BCA assay (bicinchoninic acid assay, Sigma-Aldrich). All measurements were done in triplicate.

**Sialidase analysis.** The assay mixture (200 μL) contained horseradish peroxidase (>15 U), glucose oxidase from *Aspergillus niger* (>0.5 U), β-galactosidase from *Aspergillus oryzae* (>0.6 U) (all enzymes from Sigma-Aldrich), flavin adenine dinucleotide (0.1 mM), 4-aminoantipyrine (2.1 mM), vanillic acid (2.1 mM) and the respective substrate (4.0 mM) in sodium acetate buffer (50 mM, 5.0 mM CaCl<sub>2</sub>) at pH 5.5. Reactions were supplemented by a limiting quantity of neuraminidase (from *Clostridium perfringens*, >2 mU, Sigma-Aldrich; or from *Vibrio cholerae*, >10 mU, New England Biolabs). All assays were conducted as triplicates in 96-well plates at 35 °C and started by addition of a double-concentrated substrate solution (for competitive assays containing both substrates at double concentration).

## Acknowledgements

This work was supported by funds from the State of Hesse. Open access funding enabled and organized by Projekt DEAL.

## References

- [1] R. Schauer, *Glycoconjugate J.* **2000**, *17*, 485–499.
- [2] A. Varki, R. Schauer, *Essentials of Glycobiology (2nd ed.)*. Cold Spring Harbor Laboratory Press **2009**, 199–227.
- [3] T. Angata, A. Varki, *Chem. Rev.* **2002**, *102*, 439–469.
- [4] Y. A. Knirel, A. S. Shashkov, Y. E. Tsvetkov, P.-E. Jansson, U. Zaehring, *Adv. Carbohydr. Chem. Biochem.* **2003**, *58*, 371–417.
- [5] A. L. Lewis, N. Desa, E. E. Hansen, Y. A. Knirel, J. I. Gordon, P. Gagneux, V. Nizet, A. Varki, *Proc. Natl. Acad. Sci. USA* **2009**, *106*, 13552–13557.
- [6] A. Varki, *Nature* **2007**, *446*, 1023–1029.
- [7] H. Laubli, A. Varki, *Cell. Mol. Life Sci.* **2019**.
- [8] A. Varki, *Trends Mol. Med.* **2008**, *14*, 351–360.
- [9] P. R. Crocker, J. C. Paulson, A. Varki, *Nature Rev. Immunol.* **2007**, *7*, 255–266.
- [10] O. Blixt, S. Han, L. Liao, Y. Zeng, J. Hoffmann, S. Futakawa, J. C. Paulson, *J. Am. Chem. Soc.* **2008**, *130*, 6680–6681.
- [11] N. R. Zaccai, K. Maenaka, T. Maenaka, P. R. Crocker, R. Brossmer, S. Kelm, E. Y. Jones, *Structure* **2003**, *11*, 557–567.
- [12] B. E. Collins, O. Blixt, S. Han, B. Duong, H. Li, J. K. Nathan, N. Bovin, J. C. Paulson, *J. Immunol.* **2006**, *177*, 2994–3003.
- [13] H. Prescher, A. Schweizer, E. Kuhfeldt, L. Nitschke, R. Brossmer, *ACS Chem. Biol.* **2014**, *9*, 1444–1450.
- [14] C. D. Rillahan, M. S. Macauley, E. Schwartz, Y. He, R. McBride, B. M. Arlian, J. Rangarajan, V. V. Fokin, J. C. Paulson, *Chem. Sci.* **2014**, *5*, 2398–2406.
- [15] Y. Zeng, C. Rademacher, C. M. Nycholat, S. Futakawa, K. Lemme, B. Ernst, J. C. Paulson, *Bioorg. Med. Chem. Lett.* **2011**, *21*, 5045–5049.
- [16] C. D. Rillahan, E. Schwartz, C. Rademacher, R. McBride, J. Rangarajan, V. V. Fokin, J. C. Paulson, *ACS Chem. Biol.* **2013**, *8*, 1417–1422.
- [17] C. D. Rillahan, E. Schwartz, R. McBride, V. V. Fokin, J. C. Paulson, *Angew. Chem. Int. Ed.* **2012**, *51*, 11014–11018.
- [18] M. von Itzstein, *Nat. Rev. Drug Discovery* **2007**, *6*, 967–974.
- [19] M. E. Giorgi, R. M. de Lederkremer, *Carbohydr. Res.* **2011**, *346*, 1389–1393.
- [20] S. Quosdorf, A. Schuetz, H. Kolodziej, *Molecules* **2017**, *22*, 1989/1981–1989/1918.
- [21] X. Chen, A. Varki, *ACS Chem. Biol.* **2010**, *5*, 163–176.
- [22] W.-D. Fessner, N. He, D. Yi, P. Unruh, M. Knorst, in *Cascade Biocatalysis* (Eds.: S. Riva, W.-D. Fessner), Wiley-VCH, Weinheim, **2014**, pp. 361–392.
- [23] L. Deng, X. Chen, A. Varki, C. A. Bush, *Biopolymers* **2013**, *99*, 650–665.
- [24] M. Knorst, W.-D. Fessner, *Adv. Synth. Catal.* **2001**, *343*, 698–710.
- [25] N. He, D. Yi, W.-D. Fessner, *Adv. Synth. Catal.* **2011**, *353*, 2384–2398.
- [26] D. Yi, N. He, M. Kickstein, J. Metzner, M. Weiss, A. Berry, W.-D. Fessner, *Adv. Synth. Catal.* **2013**, *355*, 3597–3612.
- [27] A. Mertsch, N. He, D. Yi, M. Kickstein, W.-D. Fessner, *Chem. Eur. J.* **2020**, *26*, 11614–11624.
- [28] C.-J. Li, T.-H. Chan, *Tetrahedron* **1999**, *55*, 11149–11176.
- [29] Z.-L. Shen, S.-Y. Wang, Y.-K. Chok, Y.-H. Xu, T.-P. Loh, *Chem. Rev.* **2013**, *113*, 271–401.
- [30] M. Warwel, W.-D. Fessner, *Synlett* **2002**, 2104–2106.
- [31] P. A. Veronesi, P. E. A. Rodriguez, E. Peschechera, S. L. Veronesi, **2008**, WO2008/090151.
- [32] E. Kim, D. M. Gordon, W. Schmid, G. M. Whitesides, *J. Org. Chem.* **1993**, *58*, 5500–5507.
- [33] L. A. Paquette, P. C. Lobben, *J. Am. Chem. Soc.* **1996**, *118*, 1917–1930.

- [34] L. A. Paquette, T. M. Mitzel, *J. Am. Chem. Soc.* **1996**, *118*, 1931–1937.
- [35] P. Allevi, P. Rota, R. Scaringi, R. Colombo, M. Anastasia, *J. Org. Chem.* **2010**, *75*, 5542–5548.
- [36] A. Xiao, T. J. Slack, Y. Li, D. Shi, H. Yu, W. Li, Y. Liu, X. Chen, *J. Org. Chem.* **2018**, *83*, 10798–10804.
- [37] W. Li, T. Ghosh, Y. Bai, A. Santra, A. Xiao, X. Chen, *Carbohydr. Res.* **2019**, *479*, 41–47.
- [38] I. M. Morrison, M. B. Perry, *Can. J. Biochem.* **1966**, *44*, 1115.
- [39] T. Woodhall, G. Williams, A. Berry, A. Nelson, *Angew. Chem. Int. Ed.* **2005**, *44*, 2109–2112.
- [40] A. Kinnell, T. Harman, M. Bingham, A. Berry, A. Nelson, *Tetrahedron* **2012**, *68*, 7719–7722.
- [41] S. Kelm, P. Madge, T. Islam, R. Bennett, H. Koliwer-Brandl, M. Waespy, M. von Itzstein, T. Haselhorst, *Angew. Chem. Int. Ed.* **2013**, *52*, 3616–3620.
- [42] R. Willand-Charnley, T. J. Fisher, B. M. Johnson, P. H. Dussault, *Org. Lett.* **2012**, *14*, 2242–2245.
- [43] K. Abiraj, D. C. Gowda, *J. Chem. Res.* **2003**, 332–334.
- [44] T. Tsuchiya, M. Nakano, T. Torii, Y. Suzuki, S. Umezawa, *Carbohydr. Res.* **1985**, *136*, 195–206.
- [45] M. Kouhkan, B. Zeynizadeh, *Bull. Korean Chem. Soc.* **2011**, *32*, 3323–3326.
- [46] S. C. Mosimann, M. Gilbert, D. Dombrowski, R. To, W. Wakarchuk, N. C. J. Strynadka, *J. Biol. Chem.* **2001**, *276*, 8190–8196.
- [47] S. Krapp, A. K. Munster-Kuehnel, J. T. Kaiser, R. Huber, J. Tiralongo, R. Gerardy-Schahn, U. Jacob, *J. Mol. Biol.* **2003**, *334*, 625–637.
- [48] D. C. Watson, S. Leclerc, W. W. Wakarchuk, N. M. Young, *Glycobiology* **2011**, *21*, 99–108.
- [49] M. Potier, L. Mameli, M. Belisle, L. Dallaire, S. B. B. Melancon, *Anal. Biochem.* **1979**, *94*, 287–296.
- [50] K. E. Achyuthan, A. M. Achyuthan, *Comp. Biochem. Physiol. Part B* **2001**, *129B*, 29–64.
- [51] Y. V. Sheludko, W.-D. Fessner, *Curr. Opin. Struct. Biol.* **2020**, *63*, 123–133.
- [52] Z. Khedri, M. M. Muthana, Y. Li, S. M. Muthana, H. Yu, H. Cao, X. Chen, *Chem. Commun.* **2012**, *48*, 3357–3359.